

Cite this: *Soft Matter*, 2011, **7**, 3482

www.rsc.org/softmatter

PAPER

# Study of poly(*N,N*-diethylacrylamide) nanogel formation by aqueous dispersion polymerization of *N,N*-diethylacrylamide in the presence of poly(ethylene oxide)-*b*-poly(*N,N*-dimethylacrylamide) amphiphilic macromolecular RAFT agents†

Chloé Grazon,<sup>ab</sup> Jutta Rieger,<sup>\*a</sup> Nicolas Sanson<sup>b</sup> and Bernadette Charleux<sup>c</sup>

Received 21st October 2010, Accepted 12th January 2011

DOI: 10.1039/c0sm01181a

The formation of thermoresponsive poly(*N,N*-diethylacrylamide) (PDEAAm) nanogels *via* an aqueous dispersion polymerization process in the presence of poly(ethylene oxide)-*b*-poly(*N,N*-dimethylacrylamide) macromolecular reversible addition–fragmentation chain transfer agents (macroRAFT agents) was studied. The latter exhibit a hydrophobic trithiocarbonate reactive group with a dodecyl substituent, and had previously proved to act simultaneously as control agents and stabilizers in such a synthesis process (Rieger *et al.*, *J. Polym. Sci. Part A: Polym. Chem.*, 2009, **47**, 2373). The nanogel size and stability were found to depend strongly on the chain length of the macroRAFT agents, but also on the crosslinker (*N,N*-methylene bisacrylamide) and monomer concentrations. The aim of the present work was to better understand the mechanisms that govern the nanogel formation in such heterogeneous polymerization conditions performed under RAFT control, with special emphasis on the role of the macroRAFT agents. In the first part, the aqueous solution properties of the macroRAFT agents in the conditions of the dispersion polymerizations were studied by light scattering and fluorescence spectroscopy and it was found that they self-assemble to form star micelles. In the second part, the nanogel formation at different DEAAm and crosslinker concentrations was monitored by dynamic and static light scattering, and by size exclusion chromatography. It appeared that at low monomer conversion the calculated number of chains per nanogel particle was close to the aggregation number,  $N_{\text{agg}}$ , of the macroRAFT agent micelles. With increasing conversions, however, the number of chains clearly increased and exceeded the initial  $N_{\text{agg}}$ . Higher monomer concentrations hardly influenced the formation process and thus the gel particle size, whereas enhanced crosslinker concentration had a strong impact on the latter. These results strongly suggest that precursor particles are formed very rapidly at the polymerization onset and then aggregate with each other to form complex inter-crosslinked particles.

## Introduction

Nanogels have been defined as gel particles with diameters below 100 nm exhibiting network structure that swell in a suitable solvent.<sup>1</sup> They have received considerable interest for applications in various areas including materials science,<sup>2,3</sup> drug delivery,<sup>4,5</sup> and biosensors,<sup>6</sup> due to their unique physical and chemical properties. Especially nanogels coated by poly(ethylene oxide) (PEO) chains have attracted attention as PEO is biocompatible and provides colloidal stability.<sup>5,7</sup> A simple synthesis approach relies on radical crosslinking copolymerization (RCC) of a vinyl monomer with a bifunctional monomer (crosslinker) performed in highly diluted solution. In the last decade, significant advances in the synthetic pathways (polymerization techniques and processes) have been made that allow not only the chemical composition of those crosslinked polymer

<sup>a</sup>Laboratoire de Chimie des Polymères, UPMC Sorbonne Universités and CNRS, UMR 7610, 3 rue de Galilée, 94200 Ivry, France. E-mail: jutta.rieger@upmc.fr

<sup>b</sup>Laboratoire de Physico-chimie des Polymères et Milieux Dispersés, UMR 7615 UPMC-CNRS-ESPCI, Ecole Supérieure de Physique et de Chimie Industrielles ESPCI, 10 rue Vauquelin, 75231 Paris Cedex 05, France

<sup>c</sup>Université de Lyon, Université Lyon 1, CPE Lyon, CNRS UMR 5265, C2P2, Team LCPP Bat 308F, 43 Bd du 11 novembre 1918, 69616 Villeurbanne, France

† Electronic supplementary information (ESI) available: Additional supporting information including a comparison of the evolutions of the aggregation number of macroRAFT agent micelles and the hydrodynamic diameters of the nanogel, <sup>1</sup>H-NMR analysis showing the individual consumption of DEAAm and the crosslinker during polymerization, and size exclusion chromatograms. See DOI: 10.1039/c0sm01181a

particles to be tuned, but also their size, morphology and functionality.<sup>7,8</sup> Today's trends pass on to heterogeneous polymerization processes, that may allow for syntheses to be performed in water at higher monomer concentration (compared to solution polymerization) as the polymerization is performed in a confined nanometric space.<sup>7,9,10</sup> In addition, the application of controlled radical polymerization (CRP) techniques (atom transfer radical polymerization, ATRP,<sup>11,12</sup> nitroxide mediated polymerization, NMP,<sup>13,14</sup> reversible addition–fragmentation chain transfer, RAFT,<sup>15–18</sup> macromolecular design *via* the interchange of xanthates, MADIX<sup>19–21</sup>) limits chain growth, and paves the way to a good control over the nanogel size.<sup>7</sup> Especially the RAFT/MADIX technique, which is one of the most versatile CRP technique, has provided encouraging results in the synthesis of nanogels. Using macromolecular RAFT agents (macroRAFT agents) based on PEO, Yan and Tao recently prepared cationic poly(*N,N*-dimethylaminoethyl methacrylate)-based nanogels in acidic aqueous solution.<sup>22</sup> The syntheses were performed in the presence of 3–4 mol% of crosslinker using high macroRAFT agent concentrations, *i.e.* low  $[\text{monomer}]_0/[\text{macroRAFT}]_0$  ratios (generally, below 25). Polymerizations performed at monomer concentration beyond 0.3 M led, however, to macrogel formation.<sup>22</sup> In heterogeneous conditions, by aqueous dispersion RAFT polymerization, Hawker *et al.*<sup>17</sup> prepared thermosensitive poly(*N*-isopropylacrylamide) nanogels stabilized by poly(*N,N*-dimethylacrylamide) chains of different length. The size and the colloidal stability of the gel particles were controlled by both the concentration and the lengths of the macromolecular RAFT agent. Again, RCC was performed using low monomer concentrations (0.15 M, monomer content in water: 1.7 wt%) and low crosslinker concentration (2 mol% based on the overall monomer concentration). Hence, one would expect that the phase separation which occurs during polymerization may allow the RCC to be performed at higher monomer concentration. It was, however, reported that a second polymerization step was necessary to reach higher solids content.<sup>17</sup> Several recent papers focused on the comprehension of nanogel formation in CRP conditions, highlighting the importance of intermolecular *vs.* intramolecular crosslinking reactions.<sup>21,23</sup> Nevertheless, the mechanisms during nanogel formation in heterogeneous conditions are still not well-understood.

We recently reported the synthesis of pegylated thermoresponsive core–shell nanogels *via* a RAFT-mediated aqueous dispersion polymerization process.<sup>18</sup> Technically, the copolymerization of *N,N*-diethylacrylamide (DEAAm) with *N,N'*-methylene bisacrylamide (MBA) was conducted at 70 °C (*i.e.* above the lower critical solution temperature, LCST, of PDEAAm) in the presence of poly(ethylene oxide)-*b*-poly(*N,N*-dimethylacrylamide) macroRAFT agents end-capped by a trithiocarbonate reactive group (PEO-*b*-PDMAAm–TTC). Upon chain extension of the latter with the hydrophobic polymer, microphase separation takes place and core-crosslinked PDEAAm particles self-stabilized by PEO-*b*-PDMAAm chains form. The stability and size of the particles were found to depend strongly on the reaction conditions and on the macroRAFT agent chain length. In optimal conditions, high solids content up to 12 wt% and nanogel particles with good colloidal stability could be reached.

The aim of the present work is to better understand the mechanisms that govern the formation of those thermosensitive

PDEAAm nanogels in aqueous dispersed phase and to elucidate the role of the PEO-*b*-PDMAAm–TTC macroRAFT agents in the process. These trithiocarbonate macromolecular RAFT agents are end-capped by a hydrophobic dodecyl (C<sub>12</sub>) chain, which might induce their self-assembly in aqueous medium.<sup>24</sup> The properties of the amphiphilic macroRAFT agents in aqueous solution were thus analyzed by light scattering and fluorescence spectroscopy before polymerization. Then, the formation of the nanogels in the presence of such macroRAFT agents was studied by dynamic and static light scattering (DLS and SLS) and size exclusion chromatography (SEC), at different monomer and crosslinker concentrations. These analyses provided important keys to the understanding of nanogel formation in an aqueous dispersed system.

## Experimental

### Materials

2,2'-Azobis(2-amidinopropane) dihydrochloride (V50, 99.9%, Aldrich), *N,N'*-methylene bisacrylamide (MBA, 97%, Alfa Aesar), and solvents were used as received. Deionized water was used for the nanogel syntheses. *N,N*-Diethylacrylamide (DEAAm) was synthesized below 10 °C in dry tetrahydrofuran (THF, VWR Normapur) by reaction of acryloyl chloride (96%, Alfa Aesar) with a twofold excess of diethylamine (>99%, Acros).<sup>18</sup> The molecular RAFT agent *S*-1-dodecyl-*S'*-( $\alpha,\alpha'$ -dimethyl- $\alpha''$ -acetic acid) trithiocarbonate (TTCA),<sup>25</sup> and the TTCA-based macromolecular RAFT agents, PEO–TTC ( $M_n = 2420 \text{ g mol}^{-1}$ , end-functionality >95%),<sup>24</sup> and PEO-*b*-PDMAAm–TTC (characteristics *cf.* Table 1)<sup>18</sup> were synthesized as reported before.

### Synthesis of pegylated PDEAAm thermosensitive nanogels by radical crosslinking dispersion copolymerization of DEAAm and MBA in the presence of living PEO-*b*-PDMAAm–TTC in water

Radical crosslinking dispersion copolymerization of DEAAm and MBA was performed in water at 70 °C in the presence of living poly(ethylene oxide)-*b*-poly(*N,N*-dimethylacrylamide) copolymers, PEO-*b*-PDMAAm–TTC.<sup>18</sup> In a typical experiment (Table 2, **S3CL3**), 363 mg of PEO-*b*-PDMAAm–TTC macroRAFT agent **M4bis** (Table 1,  $M_n = 9950 \text{ g mol}^{-1}$ ,  $3.6 \times 10^{-5} \text{ mol}$ ), 892 mg DEAAm ( $7.0 \times 10^{-3} \text{ mol}$ ) and 33 mg MBA ( $2.1 \times 10^{-4} \text{ mol}$ ) were dissolved in 29.5 mL of water, in a septum-sealed flask. Then, 56 mg of 1,3,5-trioxane ( $6.3 \times 10^{-4} \text{ mol}$ , an internal reference for the <sup>1</sup>H-NMR determination of the monomer consumption in D<sub>2</sub>O) and 0.5 mL of a  $1.4 \times 10^{-2} \text{ M}$  aqueous stock solution of V50 were added. The solution was purged with nitrogen for 30 min in an ice bath, and then placed in an oil bath thermostated at 70 °C to initiate the polymerization. Sampling was performed at regular time intervals. Conversion was nearly complete after 29 min, and the reaction was stopped by immersion of the flask in iced water. Syntheses of nanogels at higher monomer concentration (wt%) ( $S = [m_{\text{MBA}} + m_{\text{DEAAm}}]/m_{\text{total}} \times 100$ ) and/or higher crosslinker molar percentage ( $CL = n_{\text{MBA}}/[n_{\text{MBA}} + n_{\text{DEAAm}}] \times 100$ ) were performed following the same procedure. The sample composition is indicated in the sample name, for example, PEO-*b*-PDMAAm-*b*-P(DEAAm-*co*-MBA) (DEAAm/MBA: 97/3) synthesized at 3 wt% monomer

**Table 1** Characteristics of the PEO-*b*-PDMAAm-TTC macroRAFT agents

Entry	$M_n$ NMR <sup>a</sup> /g mol <sup>-1</sup>	$M_n$ SEC <sup>b</sup> /g mol <sup>-1</sup>	$M_w/M_n$ <sup>b</sup>	DP <sub>PDMAAm</sub> <sup>a</sup>	dn/dc <sup>c</sup> /mL g <sup>-1</sup>	cac <sup>d</sup> /mmol L <sup>-1</sup>	$R_h$ <sup>e</sup> /nm	$N_{agg}$ <sup>e</sup>
PEO-TTC	2400	3200	1.07	0	0.141	—	6.1	49
M1	3600	4900	1.07	12	0.140	0.13	5.5	27
M2	6000	7700	1.13	36	0.144	0.16	6.8	18
M3	8200	9600	1.14	58	0.144	0.30	7.5	15
M4	9200	11 100	1.18	68	0.152	0.27	8.2	14
M4bis	9950	11 400	1.14	—	—	—	—	—
M5	11 600	14 000	1.11	93	0.151	—	9.0	13

<sup>a</sup> Calculated number-average molar mass ( $M_n$ ) and degree of polymerization (DP<sub>PDMAAm</sub>) of the PDMAAm block for the PEO-*b*-PDMAAm-TTC diblock copolymers, where  $M_n$  and DP<sub>n</sub> of the PDMAAm block were determined from the DMAAm conversion by <sup>1</sup>H-NMR, with  $M_n$  of the PEO = 2420 g mol<sup>-1</sup>. <sup>b</sup>  $M_n$  and  $M_w/M_n$  determined by size exclusion chromatography (SEC) in DMF (+LiBr) with PMMA calibration. <sup>c</sup> Refractive index increment (dn/dc) of the PEO-*b*-PDMAAm-TTC diblock copolymers determined in water at room temperature. <sup>d</sup> Critical aggregation concentrations were determined by fluorescence spectroscopy using pyrene as probe. <sup>e</sup> Hydrodynamic radii ( $R_h$ ) and aggregation number ( $N_{agg}$ ) of the macroRAFT agent micelles determined by light scattering at 25 °C and 90°.

**Table 2** Radical Crosslinking Copolymerizations of *N,N*-diethylacrylamide (DEAAm) and *N,N'*-methylene bisacrylamide (MBA) in the presence of PEO-*b*-PDMAAm-TTC macroRAFT Agent M4 in water at 70 °C ([DEAAm + MBA]<sub>0</sub>/[M4]<sub>0</sub> = 200; [M4]<sub>0</sub>/[V50]<sub>0</sub> = 5)

Entry	$S^a$ /wt%	% MBA <sup>b</sup> /mol%	Time/min	$p^c$	In water at 25 °C			In DMF	
					$R_h^d$ /nm	$M_w^e \times 10^6$ /g mol <sup>-1</sup>	$R_g^f$ /nm	$M_w^f \times 10^6$ /g mol <sup>-1</sup>	$R_g^f$ /nm
S3CL3 <sup>h</sup>	3	3	7	0.02	—	—	—	0.02	12
			15	0.25	13	0.8	—	0.4	—
			19	0.87	26	4.3	26	5.5	23
			29	0.96	29	9.3	23	6.4	25
			72	1	31	—	—	7.6	26
S3CL6	3	6	7	0.15	—	—	—	—	—
			15	0.48	23	1.9	17	2.8	15
			18	0.80	30	6.6	23	10.8	24
			21	0.90	31	5.7	24	—	—
			25	0.95	35	5.5	24	—	—
			100	0.95	38	11.5	24	20.0	32
S3CL10	3	10	15	0.20	—	—	—	1.0	10
			17	0.40	21	5.6	—	3.0	14
			20	0.58	37	13.7	49	12.0	29
			22	0.72	46	25.3	75	—	—
			25	0.75	57	25.0	75	35.3	54
			30	0.90 <sup>g</sup>	—	—	—	—	—
S10CL3 <sup>h</sup>	10	3	5	0.16	—	—	—	0.02	—
			11	0.58	17	1.2	—	1.3	13
			14	0.97	32	8.5	22	9.4	22

<sup>a</sup> Monomer concentration =  $(m_{DEAAm} + m_{MBA})/m_{total} \times 100$ . <sup>b</sup> Crosslinker (MBA) molar content =  $n_{MBA}/(n_{MBA} + n_{DEAAm}) \times 100$ . <sup>c</sup>  $p$  = overall DEAAm and MBA conversion determined by <sup>1</sup>H-NMR spectroscopy. <sup>d</sup> Hydrodynamic radius ( $R_h$ ) determined by dynamic light scattering in water at 25 °C. <sup>e</sup>  $M_w$  and  $R_g$  determined by static light scattering in water at 25 °C. <sup>f</sup> Weight-average molar mass ( $M_w$ ) and radius of gyration ( $R_g$ ) determined SEC in DMF (+LiBr) by in-line static light scattering. <sup>g</sup> Heterogeneous sample. <sup>h</sup> macroRAFT agent M4bis instead of M4 was used.

concentration is noted S3CL3 where the first digit  $X$  denotes the monomer concentration  $S$  in wt% ( $SX$ ) and the second number  $Y$  gives the molar percentage of crosslinker (CLY).

### Characterization techniques

**<sup>1</sup>H-NMR.** NMR (<sup>1</sup>H-NMR) spectra for determination of the monomer conversion were recorded in D<sub>2</sub>O at room temperature using a 200 MHz Bruker spectrometer. In general, 1,3,5-trioxane (5.1 ppm) and/or poly(ethylene oxide) signals of the macroRAFT agent (3.6 ppm) were used as internal standards and monomer conversion was determined by the relative decrease of the DEAAm and MBA signals at 5.6, 6.0–6.1, and 6.6 ppm (cf. Fig. S2 in the ESI†). The MBA conversion compared to the DEAAm conversion was determined in D<sub>2</sub>O with a 500 MHz

Bruker spectrometer by the relative decrease of the DEAAm (5.6, 6.0, and 6.6 ppm) and MBA signals (5.6 and 6.1 ppm) (cf. Fig. S2 in the ESI†). The same spectrometer was used to determine the end-functionalization of the PEO-based macroRAFT agent PEO-TTC in CDCl<sub>3</sub>. The successful removal of DMAAm in PEO-*b*-PDMAAm-TTC macroRAFT agents was demonstrated by <sup>1</sup>H-NMR in D<sub>2</sub>O with a 200 MHz Bruker spectrometer.

**SEC.** The number-average molar mass ( $M_n$ ), the weight-average molar mass ( $M_w$ ), and the polydispersity index (PDI =  $M_w/M_n$ ) were determined by size exclusion chromatography (SEC) in DMF (+LiBr, 1 g L<sup>-1</sup>) at 60 °C and at a flow rate of 0.8 mL min<sup>-1</sup>. All linear polymers were analyzed at a concentration of 5 mg mL<sup>-1</sup> in DMF (+LiBr, 1 g L<sup>-1</sup>) after filtration through 0.2 μm pore size membrane. For all experiments, the

PEO-*b*-PDMAAm–TTC macroRAFT agent concentration was determined on the basis of its  $M_n$  calculated from the  $^1\text{H-NMR}$  conversion of DMAAm after checking by SEC the complete crossover from PEO–TTC to the diblock copolymer. The weight-average molar masses,  $M_w$ , used for the light scattering calculations were estimated as follows:  $M_w = M_n (\text{NMR}) \times M_w/M_n$  (SEC), where  $M_w/M_n$  is the polydispersity index determined by SEC in DMF with a poly(methyl methacrylate) (PMMA) calibration curve. Nanogels were analyzed at a concentration between 0.6 and 2 mg mL $^{-1}$  after filtration through 0.2  $\mu\text{m}$  pore size membrane. The steric exclusion was carried out on a Polymer Laboratories Gel precolumn (50  $\times$  7.5 mm) and two Polymer Laboratories Mixed C columns (5  $\mu\text{m}$ , 300  $\times$  7.5 mm; separation limits: 200–1.9  $\times$  10 $^6$  g mol $^{-1}$ ), coupled with a refractive index (RI) detector (Viscotek, Dual 250) and a light scattering (LS) detector (MiniDawn from Wyatt Technology, laser  $\lambda = 690$  nm, 3 angles  $\theta_1 = 45^\circ$ ,  $\theta_2 = 90^\circ$ , and  $\theta_3 = 135^\circ$ ). The polydispersity indexes of the samples were derived from the RI signal by a calibration curve based on PMMA standards (Polymer Standards Service). The weight-average molar masses,  $M_w$ , and the radii of gyration,  $R_g$ , of the PEO-*b*-PDMAAm-*b*-P(DEAAm-*co*-MBA) nanogels were calculated from the LS signal with the Wyatt ASTRA v.4.90 software, using the average refractive index increment ( $dn/dc$ ) of PDMAAm, PDEAAm, and PEO in DMF at  $\lambda = 546$  nm, which are 0.081 mL g $^{-1}$ , 0.073 mL g $^{-1}$  and 0.050 mL g $^{-1}$  respectively<sup>26</sup> (with  $dn/dc = w_A(dn/dc)_A + w_B(dn/dc)_B + w_C(dn/dc)_C$ , where  $w_A$ ,  $w_B$  and  $w_C$  are the weight fractions of monomer A, B and C, respectively). The  $dn/dc$  was calculated from the DEAAm conversion given by  $^1\text{H-NMR}$ , considering the nanogels as aggregates of linear triblock PEO-*b*-PDMAAm-*b*-PDEAAm polymers, which means that MBA (crosslinker) was not included in the calculation of the  $dn/dc$ .

**Light scattering.** Dynamic light scattering (DLS) and static light scattering (SLS) measurements were performed on an ALV goniometer (ALV/CGS3) at a wavelength  $\lambda = 632.8$  nm, in combination with an ALV/LSE-5003 correlator. The wavevector  $q$  is defined as  $q = 4\pi n/\lambda \sin(\theta/2)$ , where  $n$  is the refractive index of the solution and  $\theta$  the scattering angle.

The microgels were purified by dialysis (Spectra/Por regenerated cellulose membrane with a molar mass cutoff of 12 000–14 000 Da) and lyophilization. The macroRAFT agents were purified by precipitation in petroleum ether (40–60°C) and dried under reduced pressure. For the light scattering experiments the samples were dissolved at different concentrations in water (microgels: 0.0025 wt% up to 0.01 wt%; macroRAFT agents: 0.01 wt% up to 1 wt%), equilibrated at room temperature for 4 h, and then filtered through Teflon filters of 0.2  $\mu\text{m}$  pore size to remove dust before measurement.

In the dynamic mode (DLS), which allowed the determination of the hydrodynamic radius,  $R_h$ , the time correlation function of the electric field resulting from scattered light is measured, which is a decaying function in time. This function was analyzed with a Laplace inversion program. In the limit of zero scattering angle, the decay time,  $\Gamma$ , is related to the diffusion coefficient,  $D$ , as  $\Gamma = Dq^2$ . For a translational diffusion, the hydrodynamic radius,  $R_h$ , can be calculated using the Stokes–Einstein equation:  $R_h = k_B T/6\pi\eta D$  where  $k_B$  is the Boltzmann constant,  $T$  the absolute temperature and  $\eta$  the solvent viscosity.

Static light scattering was used to determine the apparent weight-average molar mass  $M_{w,\text{app}}$  and thus  $N_{\text{agg}}$  (defined as the ratio  $(M_{w,\text{app}} \text{ micelle})/(M_w, \text{ linear macroRAFT agent chain})$  for micelles formed by the different macroRAFT agents. For the microgels, the technique was used to estimate  $M_{w,\text{app}}$  (and thus  $M_{\text{chain}}$ , cfr. equation 2) and the radius of gyration,  $R_g$ .

The Rayleigh ratio  $R$  in dilute regime of concentrations follows the general expression (eqn (1)).

$$\frac{Kc}{R} = \left( \frac{1}{M_{w,\text{app}}} + 2A_2c \right) P(q)^{-1} \quad (1)$$

where  $K = 4\pi^2 n_{\text{ref}}^2 (dn/dc)^2 / N_A \lambda^4$  with  $dn/dc$  the refractive index increment,  $N_A$  the Avogadro number, and  $n_{\text{ref}}$  the refractive index of toluene.  $A_2$  is the second virial coefficient,  $c$  the concentration (g mL $^{-1}$ ) and  $P(q)$  is the form factor, which can be expressed in the Guinier regime as follows:  $P(q)^{-1} = 1 + q^2 R_g^2/3$ . For the determination of  $M_{w,\text{app}}$  and  $R_g$  of the microgels, measurements were performed at 12 different angles (from 30 to 150°). In contrast for smaller particles, *i.e.* the macroRAFT agents micelles, the form factor  $P(q)$  reduces to 1 and the general expression becomes  $Kc/R = 1/M_{w,\text{app}} + 2A_2c$  (Debye equation). Here, light scattering measurements were performed at a single scattering angle of 90°. The refractive index increments  $dn/dc$  of the macroRAFT agents (values in Table 1) and the microgels (0.17 mL g $^{-1}$ ) in aqueous solution were measured on a SpectraSystem RI-150 differential refractometer at room temperature.

**TEM.** The samples were diluted in water prior to analysis and then deposited on a carbon-coated copper grid. Uranyl acetate at 2% in water was used as contrast agent. Conventional transmission electron microscopy (TEM) was performed on a JEOL JEM CX II UHR microscope operating at 100 keV and equipped with a Keen View CCD camera from Soft Imaging System (Olympus) calibrated with three polystyrene particle samples (PELCO 610-SET—91, 300, and 482 nm, Ted Pella Inc.). The acquisition was done with the iTEM software from Soft Imaging System (Olympus).

**Fluorescence spectroscopy.** Fluorescent spectra (emission) were recorded on a Varian, Cary Eclipse fluorimeter, using the Cary Eclipse Scan Application. Samples were prepared in 10 mm fluorescence cells (Varian). 30  $\mu\text{L}$  of 1 mM ethanolic solution of pyrene was added to different macroRAFT agents' solutions in water (0.01–1.5 wt%). The excitation wavelength was set at 270 nm (maximum absorption of pyrene). The emission spectra were recorded from 320 to 410 nm. The  $I_1/I_3$  ratio of the fluorescence intensities of the first and third vibronic peaks was calculated, which provides a method to measure the polarity of the microenvironment of pyrene at binding sites in hydrophobic microdomains. Then the critical aggregation concentration ( $c_{ac}$ ) is given by the change in the  $I_1/I_3$  ratio with the polymer concentration.

## Results and discussion

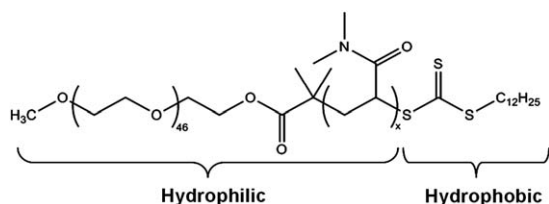
### Self-assemblies of macroRAFT agents

Before employing them in the radical crosslinking copolymerization, the behavior of the different macroRAFT agents was

investigated in aqueous solution at room temperature. Indeed, the macroRAFT agents used in this study consist of a hydrophilic polymer part composed of a block copolymer of poly(ethylene oxide) (PEO) and poly(*N,N*-dimethylacrylamide) (PDMAAm) and a hydrophobic trithiocarbonate end-group with a  $C_{12}$  alkyl chain, named PEO-*b*-PDMAAm-TTC. Despite the fact that the hydrophilic part of the PEO-*b*-PDMAAm-TTC macroRAFT agents is constituted of two distinct polymer segments, in order to simplify the discussion no difference will be made between the two polymer segments and the hydrophilic diblock copolymer will be considered as one single hydrophilic entity (Scheme 1). Due to the disparity of the length of the hydrophilic and the hydrophobic part, the macroRAFT agents look like highly asymmetric amphiphilic block copolymers that are known to self-assemble in water as star polymer micelles.<sup>27</sup>

Firstly, the critical aggregation concentrations (cac) of the synthesized macroRAFT agents were determined by fluorescence spectroscopy using pyrene as a probe. The cac values (Table 1) were all in the range of 0.1–0.3 mM, *i.e.* in the order of magnitude reported in the literature for such type of polymers.<sup>17</sup> Then, aqueous solutions of different PEO-*b*-PDMAAm-TTC macroRAFT agents were analyzed by DLS. Above the critical aggregation concentration, well-defined PEO-*b*-PDMAAm-TTC aggregates were observed, which were bigger than the macromolecular RAFT unimers and could thus be identified as assemblies of the latter. Their hydrodynamic radii,  $R_h$ , ranging between 6 and 9 nm, slightly increased with increasing PDMAAm block length (Table 1). The evolution of the hydrodynamic radii of the macroRAFT agent micelles as a function of the weight-average molar mass,  $M_w$ , of the macroRAFT agents is shown in the double-logarithmic plot in Fig. 1. When the molar mass of the macroRAFT agent increased, the hydrodynamic radii increased following a power law:  $R_h \propto M_w^{0.43}$ . Then, the aggregation number,  $N_{agg}$ , of the macroRAFT agent micelles in aqueous solution at 25 °C was determined by light scattering. The aggregation number,  $N_{agg}$ , was calculated by the ratio between the apparent weight-average molar mass of the micelle,  $M_{w,app}$ , determined by static light scattering, and the weight-average molar mass,  $M_w$ , of a single macroRAFT agent chain obtained by NMR and SEC (see Experimental part).

The dependence of the aggregation number,  $N_{agg}$ , on the weight-average molar mass of the macroRAFT agent chains,  $M_w$ , is represented in Fig. 2. It shows that  $N_{agg}$  decreases rapidly with increasing length of the hydrophilic part of the macroRAFT agent (from 49 to 13).



**Scheme 1** Representation of the macroRAFT agents, PEO-*b*-PDMAAm-TTC, constituted by a double hydrophilic poly(ethylene oxide)-*b*-poly(*N,N*-dimethylacrylamide) diblock copolymer, PEO-*b*-PDMAAm, end-capped by a hydrophobic trithiocarbonate group with a  $C_{12}$  alkyl chain.

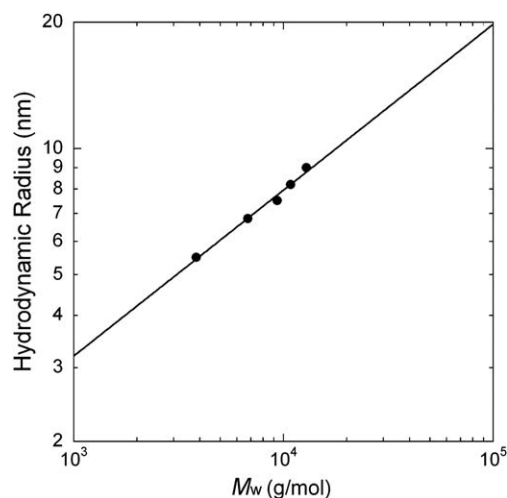


**Fig. 1** Double logarithmic representation of the hydrodynamic radius,  $R_h$ , of macroRAFT agent micelles as a function of the weight-average molar mass,  $M_w$ , of the macroRAFT agents. The full line in the double logarithmic representation indicates a power dependence  $R_h = 0.144M_w^{0.43}$  where  $R_h$  is expressed in nm and  $M_w$  in  $g\ mol^{-1}$ .

The inset in Fig. 2 displays a double logarithmic plot of  $N_{agg}$  versus  $M_w$ . It can be expressed as a power law as follows:  $N_{agg} \propto M_w^{-0.66}$ . Here, due to the particular structure of the macroRAFT agents, the power dependence cannot scale a classical model for amphiphilic block copolymers. Indeed, in a classical model  $N_{agg}$  is generally expressed as a function of the lengths of both blocks,  $N_{agg} \propto n_A^{\alpha} n_B^{\beta}$ , where  $n_A$  and  $n_B$  represent the degree of polymerization of the hydrophilic and hydrophobic block respectively.<sup>28</sup> The aggregation number generally scales with the degree of polymerization  $n_B$  of the hydrophobic block according to the power law  $N_{agg} \propto n_B^{\beta}$  where  $\beta$  was found to be 4/5.<sup>29</sup> In this study, all macroRAFT agents possess a hydrophilic block, whose length (degree of polymerization) varies, and which exhibit a short alkyl chain of constant length as hydrophobic part,

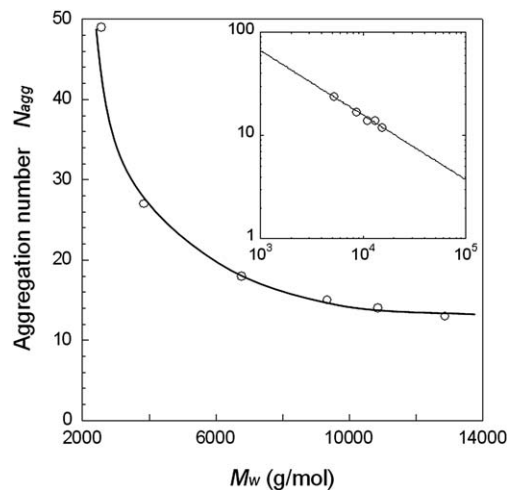


**Fig. 2** Aggregation number,  $N_{agg}$ , of the macroRAFT agent micelles as a function of the weight-average molar mass,  $M_w$ , of the macroRAFT agent chains. Inset: same variation in double logarithmic representation. The straight line corresponds to the scaling law  $N_{agg} \propto M_w^{-0.66}$ .

instead of a polymer block. Then, the above scaling relationship becomes  $N_{\text{agg}} \propto n_A^\alpha$ , and no theoretical scaling exponent could be found in the literature. However, the observed power exponent is in agreement with experimental results of Booth and Attwood<sup>30</sup> found for asymmetric poly(ethylene oxide)-*b*-poly(butylene oxide) diblock copolymers. The authors studied the effect of the length of the hydrophilic poly(ethylene oxide) block on the micellar parameters ( $R_h$  and  $N_{\text{agg}}$ ) and observed that the aggregation number decreased with increasing length of the hydrophilic block. The power law dependence with an exponent of  $-0.67$  is close to our result ( $-0.66$ , Fig. 2). As discussed above, in our system, due to the large ratio between the hydrophilic and the hydrophobic part of the macroRAFT agent, the translational diffusion of the macroRAFT agent micelles in aqueous solution is mainly governed by the large hydrophilic corona. As shown in Fig. 3, the hydrodynamic radii can be expressed as  $R_h \propto M_n^{3/5} N_{\text{agg}}^{1/5}$ . This result is in excellent agreement with the scaling law predicted by Daoud and Cotton's model for star polymer micelles in good solvent and confirms that the macroRAFT agents aggregate in the form of star polymer micelles in aqueous solution.<sup>31</sup>

As reported in our previous paper and stated in the introduction,<sup>18</sup> those living double hydrophilic diblock copolymers PEO-*b*-PDMAAm-TTC have already been successfully used in the synthesis of pegylated poly(*N,N*-diethylacrylamide) (PDEAAm) nanogels. The conditions were those of an aqueous dispersion polymerization, in which the diblock copolymer macromolecular RAFT agents played the combined role of control agent, stabilizer and surface modifier. When DLS experiments on the macroRAFT agent aqueous solutions were conducted in conditions close to those of a typical radical crosslinking copolymerization (namely at 50 °C and in the presence of DEAAm and MBA) aggregation numbers similar to those measured in water were found ( $N_{\text{agg}} = 12$  for **M4**). This means that macroRAFT agent micelles are present in the reaction media at the beginning of the polymerization. It was also found that with increasing chain length of the stabilizing double hydrophilic macroRAFT agent, the hydrodynamic diameter of

the nanogels decreased (see Fig. S1 in the ESI†).<sup>18</sup> A minimum length of the macroRAFT agent was, however, necessary to maintain the colloidal stability of the nanogels in aqueous dispersion: indeed, with the shortest polymers, stabilization was not efficient and the formation of large and polydisperse nanogels and/or aggregates occurred. In order to better understand the mechanism of formation and stabilization of the nanogels in the presence of macroRAFT agent micelles, a series of polymerizations was performed to identify more precisely their role.

### Study of nanogel formation

**Radical crosslinking copolymerization (RCC) of *N,N*-diethylacrylamide with 3 mol% of *N,N'*-methylene bisacrylamide in the presence of PEO-*b*-PDMAAm-TTC macromolecular RAFT agent (S3CL3).** Firstly, the formation of poly(*N,N*-diethylacrylamide) (PDEAAm) nanogels prepared under typical conditions<sup>18</sup> by aqueous dispersion radical polymerization at 70 °C (above the LCST of PDEAAm) in the presence of PEO-*b*-PDMAAm-TTC macroRAFT agents was studied.

They were prepared in 3 wt% DEAAm aqueous solution in the presence of 3 mol% of *N,N'*-methylene bisacrylamide (MBA) (with respect to DEAAm) (experimental results of **S3CL3** in Table 2). At the beginning of the polymerization, all components were soluble in the reaction medium. With increasing conversion, beyond a critical degree of polymerization, phase separation occurred and the medium became cloudy. Samples were taken from the reaction medium at regular time intervals, purified by dialysis and analyzed by light scattering at room temperature (25 °C, *i.e.* below the LCST of PDEAAm). The kinetics was fast in the chosen system and monomer conversion was almost complete after 22 min of polymerization affording turbid solutions at 70 °C and almost transparent solutions when cooled to room temperature. Interestingly, <sup>1</sup>H-NMR analysis of the samples (displayed in the ESI, Fig. S2†) revealed that—in the studied system—the crosslinker, MBA, was consumed only slightly more rapidly than DEAAm, indicating a quasi-simultaneous incorporation in the forming nanometric networks. Light scattering results of the purified samples in water at 25 °C showed that the hydrodynamic radius  $R_h$  of the scattering objects increased slightly with increasing monomer conversion (from 13 nm at 25% overall conversion to 31 nm at complete conversion) (Table 2). Note that the initial hydrodynamic radius of the micelles formed by PEO-*b*-PDMAAm-TTC **M4** in aqueous solution was 8.2 nm (Table 1). Simultaneously, their weight-average molar mass,  $M_w$ , increased and reached values of  $\sim 9 \times 10^6$  g mol<sup>-1</sup>. TEM microscopy of the final samples confirmed these results and showed the formation of spherical nanoparticles that were quite homogeneous in size (Fig. 4). As expected, their dimension in the dry state (TEM) was slightly smaller than the hydrodynamic radius determined in aqueous solution ( $R_{\text{TEM}} \approx 25$  nm <  $R_{h,\text{DLS}} \approx 31$  nm), due to the presence of the hydrated polymeric chains, PEO-*b*-PDMAAm, located at the nanogel surface.

In order to confirm the formation of covalently crosslinked particles, *i.e.* nanogels, rather than aggregates, the samples (without purification) were also analyzed by size exclusion chromatography (SEC) in DMF equipped with a differential refractive index (RI) detector and a static light scattering (SLS)

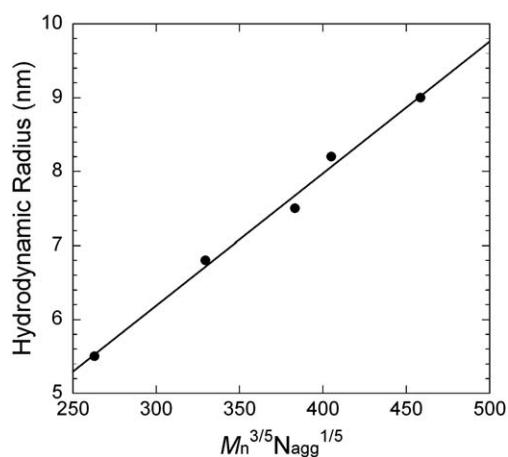


**Fig. 3** Evolution of the hydrodynamic radius,  $R_h$ , of macroRAFT agent micelles plotted as a function of  $M_n^{3/5} N_{agg}^{1/5}$ . This yields a straight line in agreement with Daoud and Cotton's predictions of the scaling theory for dimensions of star polymer micelles.<sup>31</sup>

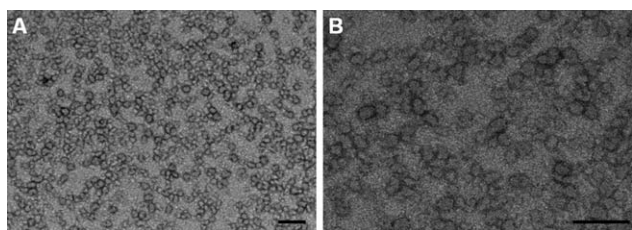


**Fig. 4** TEM micrographs of the nanogels formed in the experiment **S3CL3** dried at room temperature and negatively stained with uranyl acetate (see Table 2) at low (A) and high (B) magnification. The scale bar is 200 nm.

detector. Fig. S3 (ESI†) shows the RI signals for the PEO–TTC, the PEO-*b*-PDMAAm–TTC macroRAFT agent **M4bis** and samples obtained at different monomer conversions. The peaks' shift towards lower elution volumes indicates that the hydrodynamic diameter increased with advancing monomer conversion (consistent with the DLS results discussed earlier, Table 2), and demonstrates the formation of objects of large dimensions at the end of the polymerization. Furthermore, SEC with SLS detection allowed the determination of  $M_w$ , which was essentially in the same order of magnitude as the results obtained for purified nanogels by off-line SLS in water. It should be noted that a low quantity of chains of smaller dimensions was also detected by SEC (RI detector). They might be attributed to the presence of some non-crosslinked PEO-*b*-PDMAAm-*b*-PDEAAm triblock copolymers or residual macroRAFT agent **M4bis**. These impurities were not detected by light scattering (which is much less sensitive to objects of lower molar mass).

We have previously shown that PEO-*b*-PDMAAm–TTC macroRAFT agents are able to control the polymerization of DEAAm in aqueous dispersion yielding well-defined PEO-*b*-PDMAAm-*b*-PDEAAm triblock copolymers.<sup>18</sup> As demonstrated earlier,<sup>7,18</sup> nanogels prepared by CRP can be represented as crosslinked individual linear chains, whose length is determined by the initial  $[\text{monomer}]_0/[\text{RAFT}]_0$  ratio. In order to elucidate the mechanisms which drive the nanogel formation, we were interested in determining whether the final nanogel size is exclusively governed by the initial nucleated particle or whether particle aggregation arises during such a dispersion polymerization process. In other words, is the number of virtual linear triblock copolymer chains (*i.e.* the number of hydrophilic arms),  $N_{\text{chain}}$ , in a nanogel constant or not during polymerization, and is it related to the initial  $N_{\text{agg}}$  of the macroRAFT agent (reported in Table 1)? Knowing that the polymerization is living in equivalent conditions in the absence of crosslinker,<sup>18</sup> the following consideration can be made: if the particle formation follows a pure micellar nucleation mechanism without coagulation, the macroRAFT agent micelles initially present in the medium should yield particles composed of the same number of crosslinked triblock copolymer chains,  $N_{\text{chain}}$ , which can be calculated using eqn (2).

$$N_{\text{chain}} = \frac{M_w(\text{nanogel})}{M_w(\text{linear triblock chain})} \quad (2)$$

In eqn (2),  $M_w(\text{nanogel})$  is the weight-average molar mass of the nanogels calculated by SLS in DMF and water (Table 2), and  $M_w(\text{linear triblock chain})$  is the theoretical weight-average molar

mass of a corresponding PEO-*b*-PDMAAm-*b*-PDEAAm linear chain calculated according to eqn (3) (with  $p$  the monomer conversion reported in Table 2 and PDI = 1.25).

$$M_w(\text{linear chain}) = \left( \frac{m(\text{DEAAm} + \text{MBA})}{n(\text{macroRAFT})} \times p \times \text{PDI} \right) + M_w(\text{macroRAFT}) \quad (3)$$

The triangles in Fig. 5A represent  $M_w$  of **S3CL3** nanogels at different monomer conversions (determined by SLS in either water or DMF) as a function of the theoretically expected molar mass of a corresponding linear PEO-*b*-PDMAAm-*b*-PDEAAm

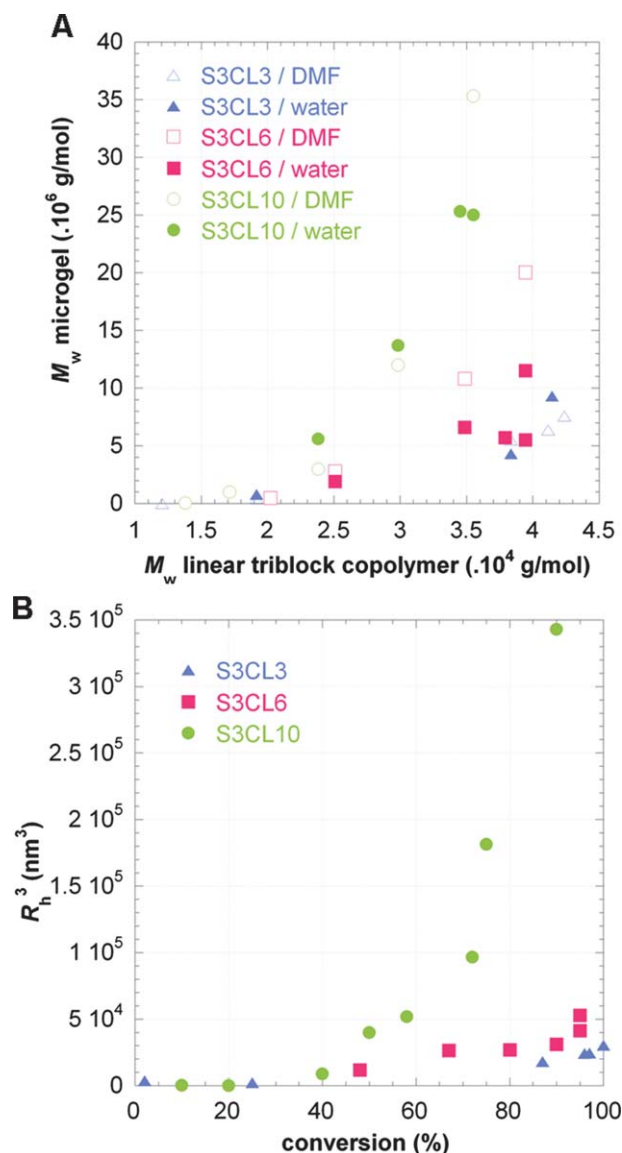


**Fig. 5** Characterization of the PDEAAm nanogels **S3CL3**, **S3CL6**, **S3CL10** synthesized with 3, 6 and 10 mol% of crosslinker respectively. (A) Evolution of the nanogels' molar masses ( $M_w$ ) determined by static light scattering in water at 25 °C (filled symbols) and DMF (+LiBr) at 50 °C (empty symbols) as a function of  $M_w$  of a corresponding linear triblock copolymer (PEO-*b*-PDMAAm-*b*-PDEAAm); (B)  $R_h^3$  representing the hydrodynamic volumes (determined by dynamic light scattering in water at 25 °C) as a function of monomer conversion.

triblock copolymer prepared in the absence of crosslinker. The slope at each point on the curve provides thus the number of virtual linear chains ( $N_{\text{chain}}$ ) corresponding to the number of macroRAFT agent chains per nanogel. In case this value is constant during polymerization a straight line should be obtained with the slope corresponding ideally to  $N_{\text{agg}}$  of the macroRAFT agent micelles (the theoretical straight line is not represented in Fig. 5A because of the very small slope in the range of 10). Hence,  $N_{\text{chain}}$  increases with increasing  $M_w$  (*i.e.* with

monomer conversion) indicating that particle aggregation takes place during polymerization.

### Study of the nanogel formation at enhanced crosslinker concentration

In order to back up the results obtained with the reference nanogel S3CL3, and to better understand the nanogel formation and the parameters that determine their final size, additional experiments were performed in the presence of higher crosslinker concentrations. The size of the resulting nanogels might indeed depend on the crosslinker concentration. Two assumptions are possible: either the enhanced amount of crosslinker will lead to the formation of denser, less swollen and potentially smaller nanogels, or bigger particles resulting from interparticle crosslinking (after aggregation of several particles) might be expected. Fig. 5B demonstrates the evolution of the nanogel dimensions (expressed as  $R_h^3$  representing the particle volume) during polymerization in the presence of three different MBA concentrations. It comes clear that the crosslinker concentration has a strong impact on the formation of the nanogels. Unlike the experiments with 3 or 6 mol% crosslinker, with 10 mol% crosslinker (S3CL10) the volume increases exponentially with the monomer conversion and the final nanogels exhibit about twice the hydrodynamic radius of those prepared with 3 and 6 mol% of crosslinker (Table 2). Note that with crosslinker concentrations above 10 mol%, macrogels were also formed. It can thus be assumed that higher crosslinker concentrations favor interparticle crosslinking. Whereas no important difference in  $R_h$  (Table 2) was stated for crosslinker concentrations of 3 and 6 mol%, SLS (Table 2) measurements revealed that the molar mass  $M_w$  of the final nanogels increased significantly with the crosslinker concentration. Fig. 5A gives access to the evolution of the average number of virtual linear chains per nanogel,  $N_{\text{chain}}$  (given by the slope), with advancing polymerization for different crosslinker concentrations. As said above, in the case of constant  $N_{\text{chain}}$  throughout the polymerization course, the nanogel molar mass would vary linearly with the individual chain molar mass. However, during the formation of the nanogels and especially for high crosslinker concentrations, we observe an exponential increase. It can clearly be observed that the higher the crosslinker concentration and the higher the monomer conversion, the steeper is the slope of the curves, *i.e.* the higher  $N_{\text{chain}}$ . From these results, it can be concluded that the crosslinker concentration affects the size and molar mass of the resulting nanogels *via* an aggregation process that appears earlier and favors the formation of bigger gel particles when the crosslinker concentration is higher. Similarly, Armes and Li studied recently the impact of crosslinker (1 mol%) in a RAFT dispersion polymerization.<sup>32</sup> It was found that the mean diameter of the particles was significantly larger in comparison to that of the particles formed in the absence of the crosslinker which is in line with our results.

### Study of the nanogel formation at enhanced monomer concentration

Finally the effect of the monomer concentration on the nanogel formation was also studied. The previous experiments were

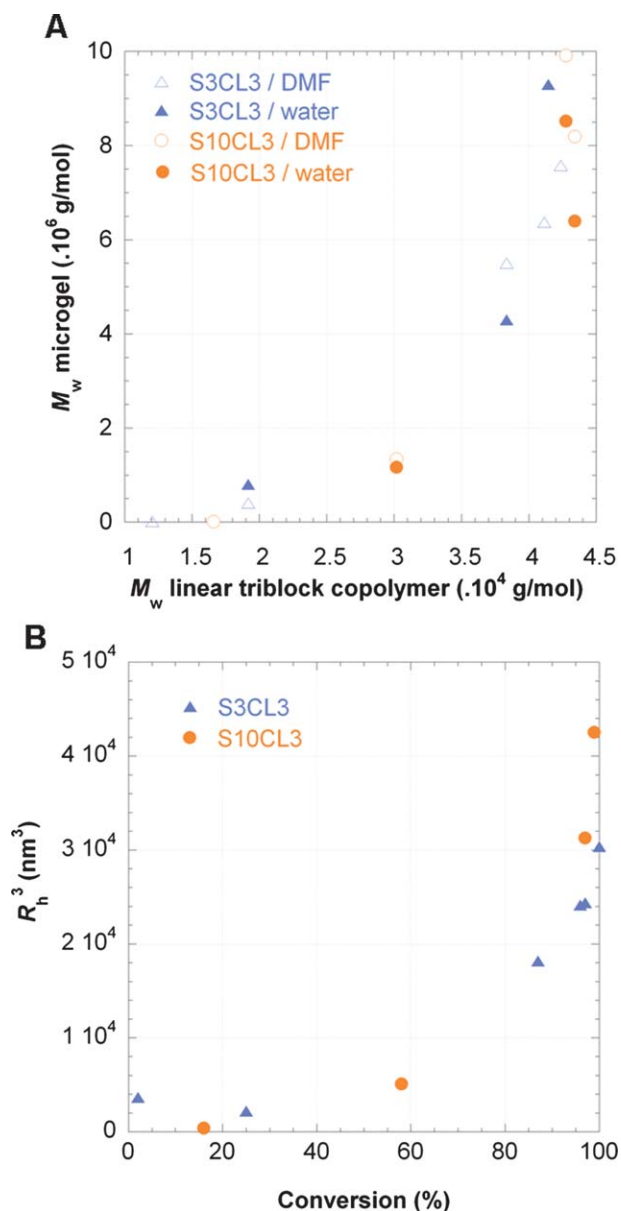


**Fig. 6** Characterization of PDEAAm nanogels synthesized at two different monomer concentrations (S3CL3 and S10CL3 with 3 wt% and 10 wt% monomer concentrations respectively). (A) Evolution of the nanogels' molar masses ( $M_w$ ) determined by static light scattering in water at 25 °C (filled symbols) and in DMF (+LiBr) at 50 °C (empty symbols), as a function of  $M_w$  of a corresponding linear triblock copolymer (PEO-*b*-PDMAAm-*b*-PDEAAm); (B)  $R_h^3$  representing hydrodynamic "volumes" (determined by dynamic light scattering in water at 25 °C) as a function of the monomer conversion.

performed at a fixed global monomer concentration of 3 wt%, corresponding to a molar monomer concentration of 0.24 mol L<sup>-1</sup> (MBA also being considered in the calculation). When the monomer concentration was enhanced to 10 wt% (0.91 mol L<sup>-1</sup>) the resulting nanogels were only slightly bigger than those prepared at 3 wt% monomer ( $R_h = 35$  nm instead of 31 nm) (Table 2, compare **S3CL3** and **S10CL3**). Regarding the formation of the nanogels (Fig. 6), only slight differences between both syntheses can be observed. The formation of big nanogels through an inter-nanogel crosslinking process is thus promoted by the crosslinker content rather than the monomer concentration. Indeed, the application of a heterogeneous polymerization process may limit the formation of macrogels or big aggregates in fairly concentrated RCC experiments provided that the concentration of the crosslinker is small.

## Conclusion

Thermoresponsive nanogels were prepared *via* a RAFT-mediated aqueous dispersion polymerization process using PEO-*b*-PDMAAm-TTC macroRAFT agents end-capped with a hydrophobic dodecyl chain. These macroRAFT agents were shown to self-assemble in aqueous solution in conditions similar to the conditions at which RCC was performed. Due to the high asymmetry of the macroRAFT agents, *i.e.* the high ratio between the hydrophilic and hydrophobic parts, the aggregates exhibit characteristics of star polymer micelles. It was found that the aggregation number  $N_{agg}$  of the macroRAFT agent micelles decreased with increasing length of the hydrophilic segment. Those macroRAFT agents were successfully employed as polymerization control agents and particle stabilizer in the aqueous dispersion crosslinking copolymerization of DEAAm and MBA. The analysis of the nanogels formation by <sup>1</sup>H-NMR, static and dynamic light scattering revealed that particle aggregation occurred during their synthesis. The extent of aggregation depended strongly on the crosslinker concentration (high crosslinker concentrations leading to large particles), and less on the monomer concentration. These results are thus a further building block to the understanding of nanogel formation in dispersed conditions.

## Acknowledgements

The authors acknowledge M. In for valuable discussions and thank J. Bellene for <sup>1</sup>H-NMR analysis on the 500 MHz NMR spectrometer (Bruker). They are also grateful to P. Beaunier for transmission electron microscopy.

## References

- 1 IUPAC, *Compendium of Chemical Terminology (the "Gold Book")*, ed. A. D. McNaught and A. Wilkinson, Blackwell Scientific Publications, Oxford, 2nd edn, 1997.
- 2 M. Das, H. Zhang and E. Kumacheva, *Annu. Rev. Mater. Res.*, 2006, **36**, 117.
- 3 L. A. Lyon, Z. Meng, N. Singh, C. D. Sorrell and A. S. John, *Chem. Soc. Rev.*, 2009, **38**, 865.
- 4 J. K. Oh, R. Drumright, D. J. Siegwart and K. Matyjaszewski, *Prog. Polym. Sci.*, 2008, **33**, 448.
- 5 A. V. Kabanov and S. V. Vinogradov, *Angew. Chem., Int. Ed.*, 2009, **48**, 5418.
- 6 J. Kim, N. Singh and L. A. Lyon, *Angew. Chem., Int. Ed.*, 2006, **45**, 1446.
- 7 N. Sanson and J. Rieger, *Polym. Chem.*, 2010, **1**, 965.
- 8 A. Blencowe, J. F. Tan, T. K. Goh and G. G. Qiao, *Polymer*, 2009, **50**, 5.
- 9 B. Charleux and F. Ganachaud, in *Macromolecular Engineering: Precise Synthesis, Materials Properties, Applications*, ed. K. Matyjaszewski, Y. Gnanou and L. Leibler, Wiley, Weinheim, 2007, vol. 1, ch. 14, pp. 605–642.
- 10 P. B. Zetterlund, Y. Kagawa and M. Okubo, *Chem. Rev.*, 2008, **108**, 3747.
- 11 J. K. Oh, C. Tang, H. Gao, N. V. Tsarevsky and K. Matyjaszewski, *J. Am. Chem. Soc.*, 2006, **128**, 5578.
- 12 J. K. Oh, D. J. Siegwart and K. Matyjaszewski, *Biomacromolecules*, 2007, **8**, 3326.
- 13 G. Delaittre, M. Save and B. Charleux, *Macromol. Rapid Commun.*, 2007, **28**, 1528.
- 14 K. I. Fukukawa, R. Rossin, A. Hagooley, E. D. Pressly, J. N. Hunt, B. W. Messmore, K. L. Wooley, M. J. Welch and C. J. Hawker, *Biomacromolecules*, 2008, **9**, 1329.
- 15 B. Liu, A. Kazlauciuonas, J. T. Guthrie and S. Perrier, *Macromolecules*, 2005, **40**, 7119.
- 16 C.-D. Vo, J. Rosselgong and S. P. Armes, *Macromolecules*, 2007, **40**, 7119.
- 17 Z. An, Q. Shi, W. Tang, C. K. Tsung, C. J. Hawker and G. D. Stucky, *J. Am. Chem. Soc.*, 2007, **129**, 14493.
- 18 J. Rieger, C. Grazon, B. Charleux, D. Alaimo and C. Jérôme, *J. Polym. Sci., Part A: Polym. Chem.*, 2009, **47**, 2373.
- 19 D. Taton, J. F. Baussard, L. Dupayage, J. Poly, Y. Gnanou, V. Ponsinet, M. Destarac, C. Mignaud and C. Pitois, *Chem. Commun.*, 2006, 1953.
- 20 J. Poly, D. J. Wilson, M. Destarac and D. Taton, *Macromol. Rapid Commun.*, 2008, **29**, 1965.
- 21 J. Poly, D. J. Wilson, M. Destarac and D. Taton, *J. Polym. Sci., Part A: Polym. Chem.*, 2009, **47**, 5313.
- 22 L. Yan and W. Tao, *Polymer*, 2010, **51**, 2161.
- 23 I. Bannister, N. C. Billingham and S. P. Armes, *Soft Matter*, 2009, **5**, 3495.
- 24 J. Rieger, F. Stoffelbach, C. Bui, D. Alaimo, C. Jérôme and B. Charleux, *Macromolecules*, 2008, **41**, 4065.
- 25 J. T. Lai, D. Filla and R. Shea, *Macromolecules*, 2002, **35**, 6754.
- 26 *Polymer Handbook*, ed. J. Brandrup, E. H. Immergut and E. A. Grulke, Wiley, 4th edn, 1999.
- 27 P. Alexandridis and B. Lindman, *Amphiphilic Block Copolymers: Self-Assembly and Applications*, Elsevier, Amsterdam, 2000.
- 28 I. W. Hamley, *The Physics of Block Copolymers*, Oxford Science Publication, 1998.
- 29 A. Halperin, *Macromolecules*, 1987, **20**, 2943.
- 30 C. Booth and D. Attwood, *Macromol. Rapid Commun.*, 2000, **21**, 501.
- 31 D. Daoud and J. P. Cotton, *J. Phys. (Paris)*, 1982, **43**, 531.
- 32 Y. Li and S. P. Armes, *Angew. Chem., Int. Ed.*, 2010, **49**, 4042.